Huffman-Coded Pulse Compression Waveforms

F. F. KRETSCHMER, JR. AND F. C. LIN

Target Characteristics Branch
Radar Division

May 23, 1985

NAVAL RESEARCH LABORATORY
Washington, D.C.

SECURITY CLASSIFICATION OF THIS PAGE

REPORT DOCUMENTATION PAGE

1a. REPORT SECURITY CLASSIFICATION UNCLASSIFIED	1b. RESTRICTIVE MARKINGS
2a. SECURITY CLASSIFICATION AUTHORITY	3. DISTRIBUTION / AVAILABILITY OF REPORT Approved for public release; distribution unlimited.
2b. DECLASSIFICATION / DOWNGRADING SCHEDULE	
4. PERFORMING ORGANIZATION REPORT NUMBER(S) NRL Report 8894	5. MONITORING ORGANIZATION REPORT NUMBER(S)
6a. NAME OF PERFORMING ORGANIZATION Naval Research Laboratory 6b. OFFICE SYMBOL (*If applicable*) 5340.1K	7a. NAME OF MONITORING ORGANIZATION Naval Sea Systems Command
6c. ADDRESS (*City, State, and ZIP Code*) Washington, DC 20375-5000	7b. ADDRESS (*City, State, and ZIP Code*) Washington, DC 20362-5101
8a. NAME OF FUNDING / SPONSORING ORGANIZATION Naval Sea Systems Command 8b. OFFICE SYMBOL (*If applicable*)	9. PROCUREMENT INSTRUMENT IDENTIFICATION NUMBER
8c. ADDRESS (*City, State, and ZIP Code*) Washington, DC 20362-5101	10. SOURCE OF FUNDING NUMBERS PROGRAM ELEMENT NO. 62712N; PROJECT NO.; TASK NO. SF12-131-001; WORK UNIT ACCESSION NO. DN-380-166
11. TITLE (*Include Security Classification*) Huffman-Coded Pulse Compression Waveforms	
12. PERSONAL AUTHOR(S) Kretschmer, F.F., Jr. and Lin, F.C.	
13a. TYPE OF REPORT Interim 13b. TIME COVERED FROM _____ TO _____	14. DATE OF REPORT (*Year, Month, Day*) 1985 May 23 15. PAGE COUNT 19
16. SUPPLEMENTARY NOTATION	

17. COSATI CODES			18. SUBJECT TERMS (*Continue on reverse if necessary and identify by block number*)
FIELD	GROUP	SUB-GROUP	Pulse compression; Low sidelobes; Match filter

19. ABSTRACT (*Continue on reverse if necessary and identify by block number*)

Radar pulse compression waveforms usually consist of constant amplitude signals whose phase or frequency is varied to obtain the desired bandwidth and sidelobe levels. However, with Huffman-coded waveforms, both the amplitude and phase vary from subpulse to subpulse. These codes are investigated in detail and compared in performance with other pulse compression waveforms.

20. DISTRIBUTION / AVAILABILITY OF ABSTRACT ☒ UNCLASSIFIED/UNLIMITED ☐ SAME AS RPT. ☐ DTIC USERS	21. ABSTRACT SECURITY CLASSIFICATION UNCLASSIFIED
22a. NAME OF RESPONSIBLE INDIVIDUAL F.F. Kretschmer, Jr.	22b. TELEPHONE (*Include Area Code*) (202) 767-3472 22c. OFFICE SYMBOL 5340.1K

DD FORM 1473, 84 MAR 83 APR edition may be used until exhausted.
All other editions are obsolete.

SECURITY CLASSIFICATION OF THIS PAGE

CONTENTS

HUFFMAN-CODED PULSE COMPRESSION WAVEFORMS

INTRODUCTION

Modern radars generally incorporate pulse compression waveforms to avoid transmitting a pulse having a large peak power which can result in waveguide arcing. Pulse compression waveforms enable one to transmit a long pulse to obtain sufficient energy on a target for detection and to simultaneously obtain the desired range resolution. This is achieved by modifying the time-bandwidth product (TB) of the transmitted waveform. A larger transmit time duration T allows sufficient energy on the target for detection, while $1/B$ determines the resolution of the compressed pulse if no mismatch occurs. The desired signal bandwidth is generally obtained by modulating the signal's phase or frequency while maintaining a constant maximum pulse amplitude. This is illustrated by the linear chirp signal, pseudorandom phase codes, and polyphase pulse compression waveforms.

A desirable property of the compressed pulse is that it have low sidelobes to prevent a weak target from being masked in the time sidelobes of a nearby stronger target. It is generally also desired that the compressed pulse does not significantly degrade when the return signal has been doppler shifted due to target motion. For the commonly used chirp signal, the sidelobes are reduced by weighting the received signal which results in a mismatch loss of approximately 1 dB, and a broadening of the pulsewidth due to the band-limiting associated with the weighting. The polyphase codes and the binary codes may also be weighted, if desired, to increase peak-to-sidelobe levels.

The Huffman-coded waveform [1 to 5] results in an ideal compressed pulse having no sidelobes except for the unavoidable sidelobe at either end of the compressed pulse. However, the Huffman waveform consists of code elements which vary in amplitude as well as in phase. Because of the amplitude fluctuations, the waveforms were not previously very practical. However, with the increased utilization of solid-state transmitters and the ability to switch the transmitters or the power transistors on and off of a transmitter bus, there has been a recent interest in investigating the properties and performance capabilities of the Huffman codes.

In this report we describe a general waveform synthesis procedure, and the synthesis of Huffman codes for a desired compressed pulse. For an N-element code, there are 2^{N-1} different uncompressed pulses having the same compressed pulse. Procedures are described for selecting an efficient Huffman code in terms of transmitted power, and the Huffman codes are compared with a polyphase code and a binary shift-register code. The effects of errors on the Huffman code sidelobes are also investigated.

WAVEFORM SYNTHESIS AND HUFFMAN CODES

A. Waveform Synthesis from a Known Compressed Pulse

We consider in the following discussion a coded transmit waveform consisting of N-subpulses which can vary in both phase and amplitude from subpulse to subpulse. This is exemplified by Barker-coded waveforms, pseudorandom binary shift-register codes, and polyphase codes. It is assumed that on reception the waveform is digitized so that an inphase I and a quadrature Q sample, or equivalently an amplitude and a phase sample, are obtained for each subpulse. This simplifies the description of the waveforms and allows us to conveniently describe the time sequence by using z-transforms. Accordingly, we denote the return sequence by $E(z)$ which is given by

Manuscript approved February 7, 1985.

$$E(z) = a_0 + a_1 z^{-1} + a_2 z^{-2} + \ldots + a_{N-1} z^{-(N-1)}, \tag{1}$$

where a_i is the complex value which specifies the amplitude and phase of the i^{th} subpulse.

A filter matched to this sequence, $M(z)$, is then given by

$$M(z) = a_{N-1}^* + a_{N-2}^* z^{-1} + a_{N-3}^* z^{-2} + \ldots + a_0^* z^{-(N-1)}. \tag{2}$$

The output of the matched filter is given by

$$G(z) = E(z)M(z) \tag{3}$$

which can be represented by

$$G(z) = g_0 + g_1 z^{-1} + g_2 z^{-2} + \ldots + g_{N-1} z^{-(N-1)} + \ldots + g_{2(N-1)} z^{-2(N-1)}, \tag{4}$$

where g_i denotes the samples of the compressed waveform.

Substituting Eqs. (1) and (2) in Eq. (3), we obtain

$$G(z) = (a_0 + a_1 z^{-1} + \ldots + a_{N-1} z^{-(N-1)})(a_{N-1}^* + a_{N-2}^* z^{-1} + \ldots + a_0^* z^{-(N-1)}). \tag{5}$$

Equation (5) can be written as

$$\begin{aligned} G(z) &= z^{-(N-1)} (a_0 + a_1 z^{-1} + \ldots + a_{N-1} z^{-(N-1)}) (a_0^* + a_1^* z + \ldots + a_{N-1}^* z^{(N-1)}) \\ &= z^{-(N-1)} E(z) E^*(1/z^*). \end{aligned} \tag{6}$$

Next, we express the z-plane zeros of $E(z)$ in factored form as

$$\prod_{i=1}^{N-1} (z - z_i), \tag{7}$$

and note from Eqs. (3) and (6) that the factored zeros of $M(z)$ may be expressed as

$$\prod_{i=1}^{N-1} (z - 1/z_i^*). \tag{8}$$

The z-plane is related to the complex S-plane by the relation

$$z = e^{ST} = e^{(\alpha + j\omega)T} = e^{\alpha T} e^{j\omega T}, \tag{9}$$

where T denotes the sampling interval or the time duration of each subpulse. From Eq. (9) it is observed that the roots of $M(z)$ given by $1/z_i^*$ are equal to the reciprocal amplitude of the roots z_i of $E(z)$, and the phase angles of the roots z_i and $1/z_i^*$ are the same. In summary, the zeros of the output function $G(z)$ occur in related pairs which are in the z-plane at the same angle but are reciprocal in amplitude. For an input N-pulse sequence there are $N-1$ such pairs of zeros.

The upshot of these relations is that the generation of the specified compressed pulse is not uniquely defined but can be accomplished by selection of either zero of each zero pair. There are 2^{N-1} possible choices of z-plane zeros that can be selected to produce the same compressed pulse. From each given choice of $(N-1)$ zeros, a different input sequence $E(z)$ can be determined from

$$E(z) = kz^{-(N-1)} \prod_{i=1}^{N-1} (z - z_i), \tag{10}$$

where k is an energy normalization constant. The resulting coefficients of the polynomial in z^{-1} specify the amplitude and the phase of the uncompressed input waveform subpulses.

These procedures are next illustrated for the well-known Barker codes having a peak-to-sidelobe power ratio that is equal to or greater than N^2. The compressed pulse for the 13-element Barker code

is shown in Fig. 1(a) on a voltage scale. From the z-transform of this response, the zero locations were determined and are shown in Fig. 1(b). It is seen that there are 12 pairs of zeros and thus 2^{12} different input waveforms which, when match-filtered, produce the same compressed pulse shown in Fig. 1(a). Each of the zeros comprising a pair are related to each other as being conjugate reciprocal zeros. For a given selection of zeros the input waveform is found from the coefficients of the polynomial resulting from performing the multiplication in Eq. (10).

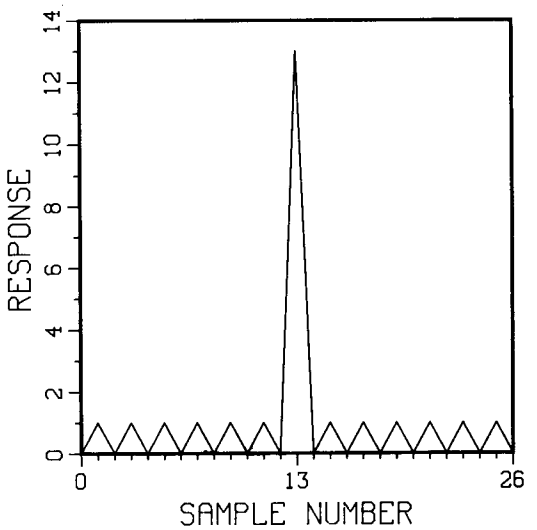

Fig. 1(a) — Compressed pulse for a 13-element Barker code

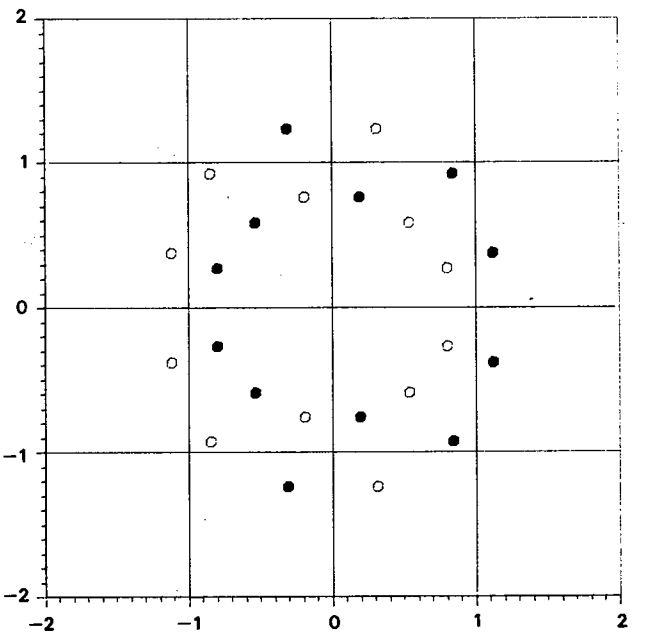

Fig. 1(b) — z-plane zero locations for a compressed 13-element Barker code

This can be efficiently and more accurately achieved using fast Fourier transform (FFT) algorithms when N becomes very large [6]. The particular set of zeros indicated by the filled-in circles corresponds to a constant amplitude binary waveform which is the well-known 13-element Barker code. In general, any other selection of zeros would result in an input waveform which varies in both amplitude and phase from subpulse to subpulse.

In Fig. 2 we show, as another example, the zeros of a compressed pulse for a four-element generalized Barker code making use of a sextic alphabet [7] whose elements consist of powers of $\exp(j\pi/3)$.

B. Huffman Codes

Huffman considered the idealized compressed pulse which contains no sidelobes except the unavoidable sidelobes at either end of the compressed pulse. The end sidelobe-level is a design parameter, and a compressed 64-element, zero-doppler Huffman code is illustrated in Fig. 3 for a relative sidelobe amplitude level of 0.1/64 V in voltage or −56 dB.

From Eq. (4) the z-transform of the compressed Huffman-coded waveform, which has been normalized to unity at the peak, takes the simple quadratic form

$$G(z) = s + z^{-(N-1)} + sz^{-2(N-1)} = s(z^{-2(N-1)} + z^{-(N-1)}/s + 1), \tag{11}$$

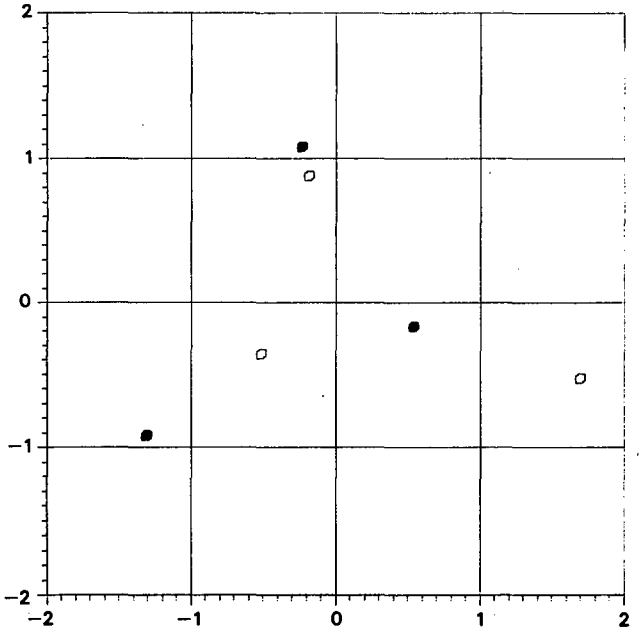

Fig. 2 — z-plane zero locations for a compressed four-element sextic code

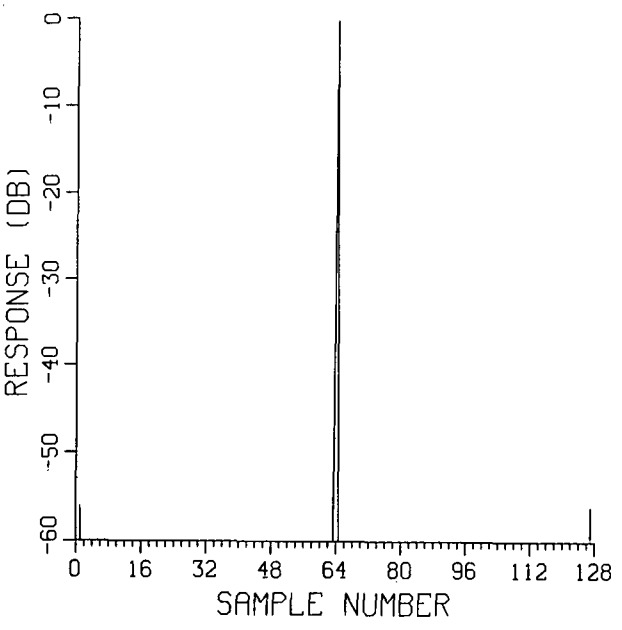

Fig. 3 — Compressed 64-element Huffman-coded waveform

where s is the normalized sidelobe voltage (that can be positive or negative). The roots of this equation lie in the z-plane at intervals of $2\pi/(N-1)$ on two circles whose radii R and R^{-1} are given by

$$\left[\left|\frac{1}{2s}\right| \pm \left(\frac{1}{4s^2} - 1\right)^{1/2}\right]^{\frac{1}{(N-1)}}. \tag{12}$$

Thus, the distinguishing feature of the zeros of the compressed Huffman code, in contrast to the other codes, is that they are on two circles whose radii are reciprocal of each other at regularly spaced intervals of $2\pi/(N-1)$ radians.

The design of a Huffman code consists of specifying the number of code elements N, the sidelobe level s, and the particular choice of z-plane zeros which results from choosing one zero from each of the 2^{N-1} pairs. In general, for given N and s, the amplitude as well as the phase of each resulting uncompressed code subpulse varies with the different choice of z-plane zeros.

DESIGN OF EFFICIENT HUFFMAN CODES

Selecting the zero pattern of $G(z)$ in a random manner to determine the input-coded waveform generally results in codes which vary considerably in amplitude from subpulse to subpulse. This represents a loss in terms of the power that could be transmitted at the maximum level. We define an efficiency factor E as the ratio of the power represented by a given Huffman-coded waveform to the power that results from transmitting a constant envelope waveform having a value equal to the largest subpulse value. This can be written as

$$E = \frac{\sum_{i=0}^{N-1} |a_i|^2}{N|a_i|^2_{\max}}. \tag{13}$$

Although stated differently, this definition is equivalent to the definition of Huffman and Ackroyd except that the maximum value of E is normalized to unity.

Ackroyd [5] proposed a method for improving the efficiency of a Huffman code based on a paper by Schroeder [8] whereby the efficiency of a waveform is improved by modifying the phase spectrum of the waveform. In particular it was found that waveforms having a high FM content tended to be efficient. Accordingly, Ackroyd cleverly determined which zero to use in each pair by noting that the pulse spectrum due to the zeros changes by plus or minus π, depending on whether the zero is inside or outside the unit circle, as one traverses the unit circle in the vicinity of the zero-pair. Ackroyd suggested that the desired zero selection could be determined by using the desired phase-spectral function as an input to a delta-modulator which provides a staircase approximation to the phase spectrum in step sizes of plus or minus π. By noting the polarity of the staircase function steps, one could identify the appropriate zero of each zero pair.

The desired phase spectrum is given by Ackroyd [5], in our notation, as

$$\arg C_n = \arg C_0 - \pi n^2/N + \pi n \qquad n = 0, 1, \ldots N-1, \tag{14}$$

where the C_n represents the Fourier coefficients of the waveform. Ackroyd [5] states that C_0 is arbitrary. However, it will be shown later that C_0 is not arbitrary in terms of the achievable efficiency. We mention at this juncture that the desirable phase characteristic given by Schroeder is very similar to the phase characteristic used in the P3 and P4 polyphase-coded waveforms devised by Lewis and Kretschmer [9,10].

To illustrate these concepts we randomly selected the zeros from the zero pairs of a 64-element Huffman code having a sidelobe voltage of -0.1 V. This was done with a computer random-number generator having equally likely plus and minus ones which were associated with a zero location inside or outside the unit circle. From these zero locations, the input waveform was determined as previously described. The amplitude distribution of this waveform is shown in Figs. 4(a) and 4(b) for different trials. The efficiencies of these waveforms are 11% and 16%. Using the method of imparting a large FM content to the waveform resulted in the waveform shown in Fig. 4(c) whose efficiency is 39%. The waveforms shown in Fig. 4 were normalized to have a compressed pulse peak equal to 64.

Ackroyd noted that the efficiency could be improved by varying the design sidelobe level. We confirmed this and in addition found that the value of C_0 in the desired characteristic given by Eq. (14) could be altered to result in a different zero selection and hence a different efficiency. The variation of the efficiency with the initial phase and the sidelobe level is shown in Fig. 5 for the 64-element Huffman code.

COMPARISON OF HUFFMAN CODES WITH OTHER CODES

We first describe and compare the 64-element Huffman code with a 64-element polyphase P4 code and a 63-element pseudorandom shift-register binary code in terms of doppler sensitivity. Next, the sensitivity of the Huffman-code sidelobes due to tolerance errors and due to finite quantization levels is presented.

The ambiguity function of an efficient 64-element Huffman code (as shown in Fig. 4(c)) having an initial phase angle of $-\pi$ and a sidelobe level of -56 dB is shown in Fig. 6. The delay is normalized to the uncompressed pulse length T, and the y-axis is the product of the doppler frequency and T. This product can also be interpreted as the number of 2π phase shifts across the uncompressed pulse due to doppler. A blowup of this figure is shown in Fig. 7 where the product of the doppler frequency and T ranges from 0 to 1. It is seen in Figs. 6 and 7 that the sidelobes of the Huffman code grow rapidly with an increase in doppler. For comparison we show the ambiguity function of a P4 code in

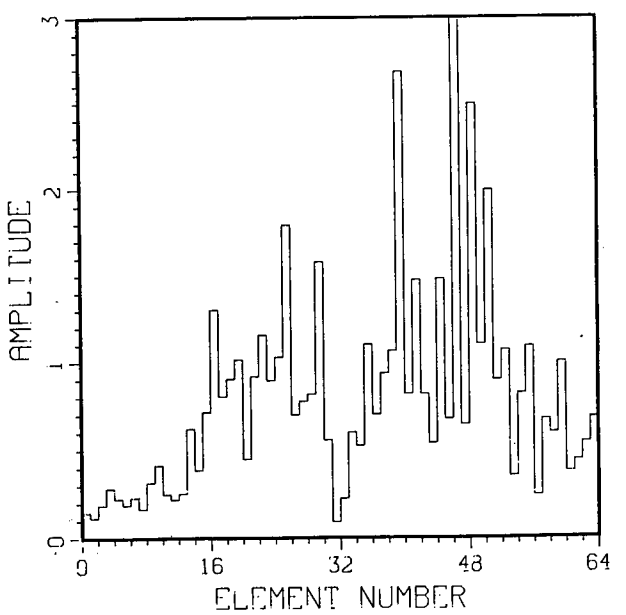

(a) efficiency is 11%

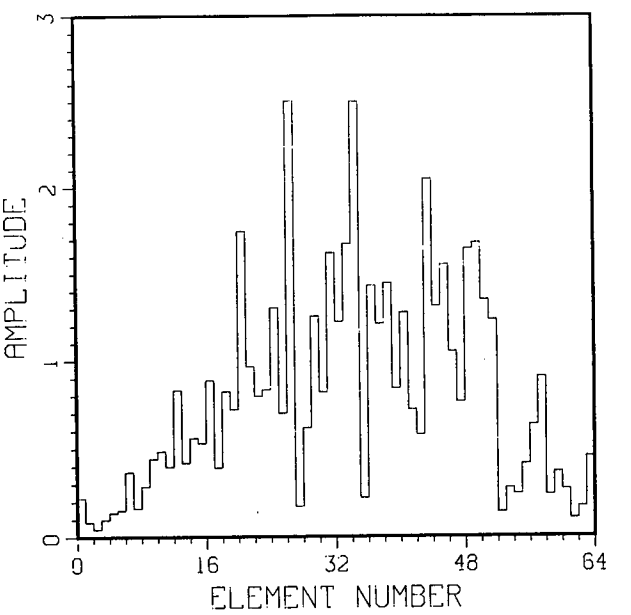

(b) efficiency is 16%

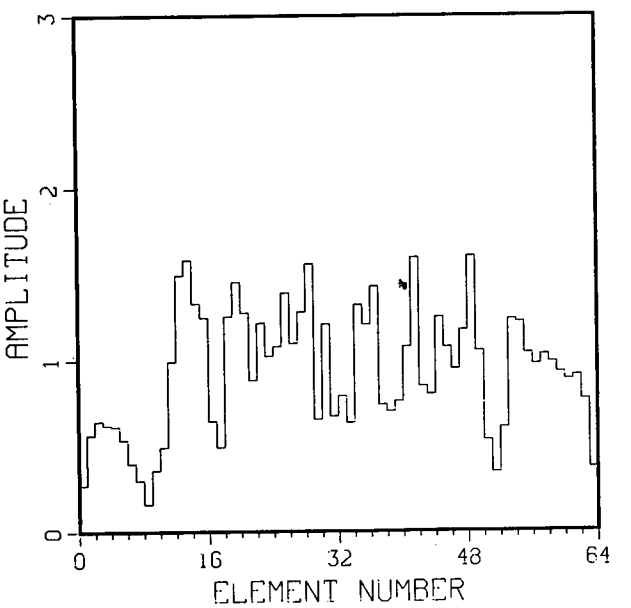

(c) efficiency is 39% due to imparting an FM phase characteristic on waveform

Fig. 4 — Amplitudes of different 64-element Huffman-coded waveforms having the same compressed pulse as shown in Fig. 3

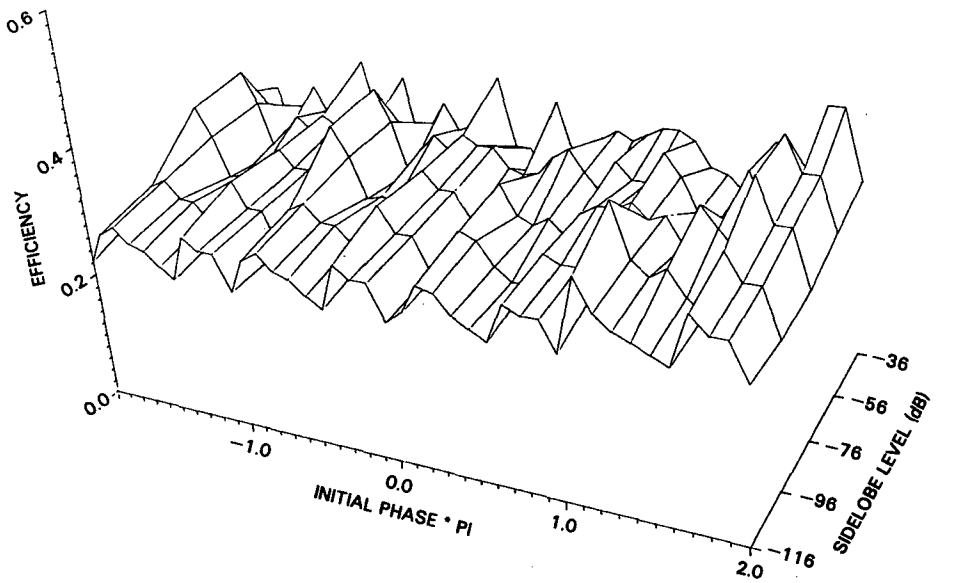

Fig. 5 — Variation of 64-element Huffman-coded waveform efficiency with the design sidelobe level and the initial phase angle of the FM pulse characteristic

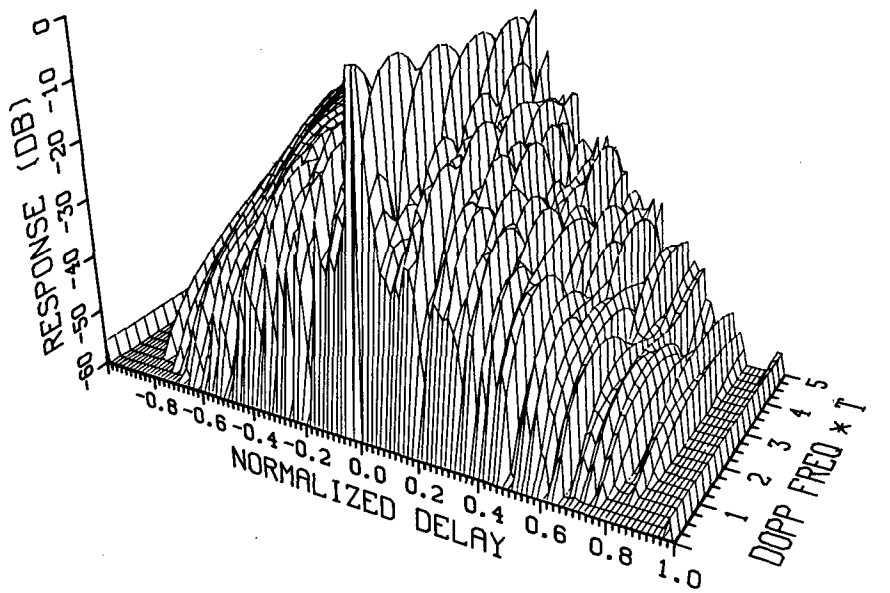

Fig. 6 — Partial ambiguity surface for an efficient 64-element Huffman-coded waveform

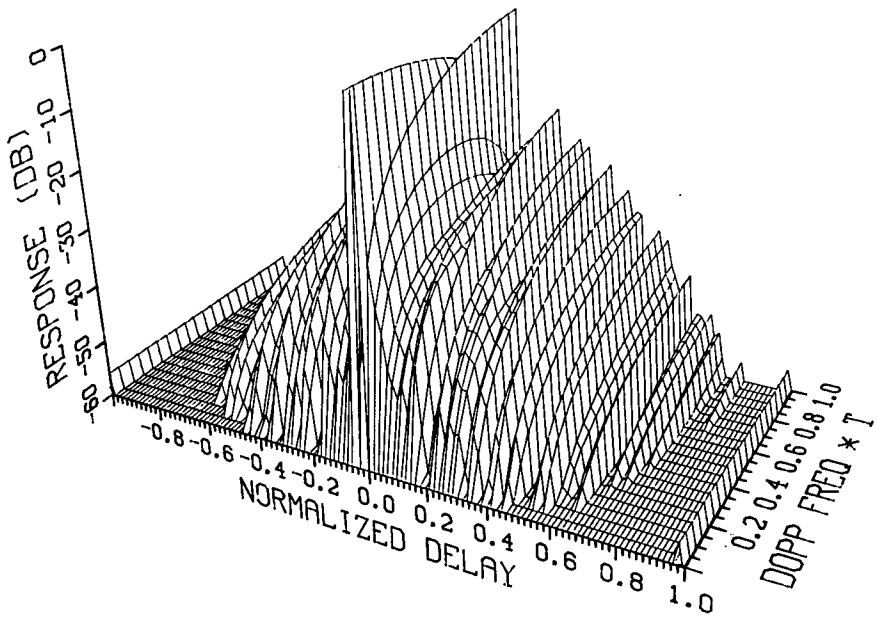

Fig. 7 — Expanded ambiguity surface for an efficient 64-element Huffman-coded waveform

Fig 8. This code, which is derived from a linear chirp signal, is seen to be relatively insensitive to doppler. Figures 9 and 10 show the ambiguity function of a 63-element pseudorandom binary shift-register code which has a thumbtack ambiguity function. Although this is an excellent waveform for simultaneous determination of range and doppler, it has a relatively poor doppler response. The response in doppler for 0-delay is approximately a $(\sin x/x)^2$ response with the first zero occurring at a normalized doppler shift of 1.0.

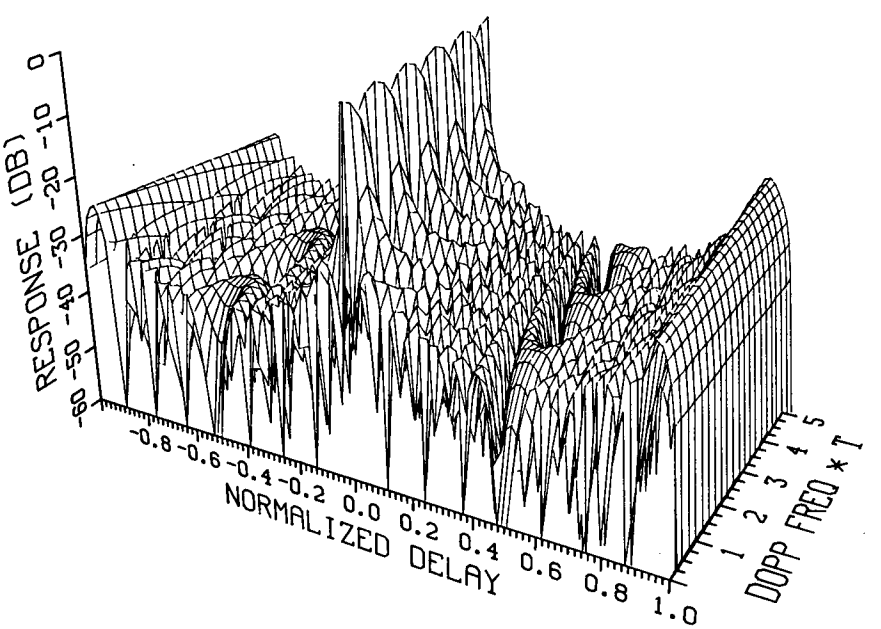

Fig. 8 — Partial ambiguity surface for a 64-element P4 polyphase-coded waveform

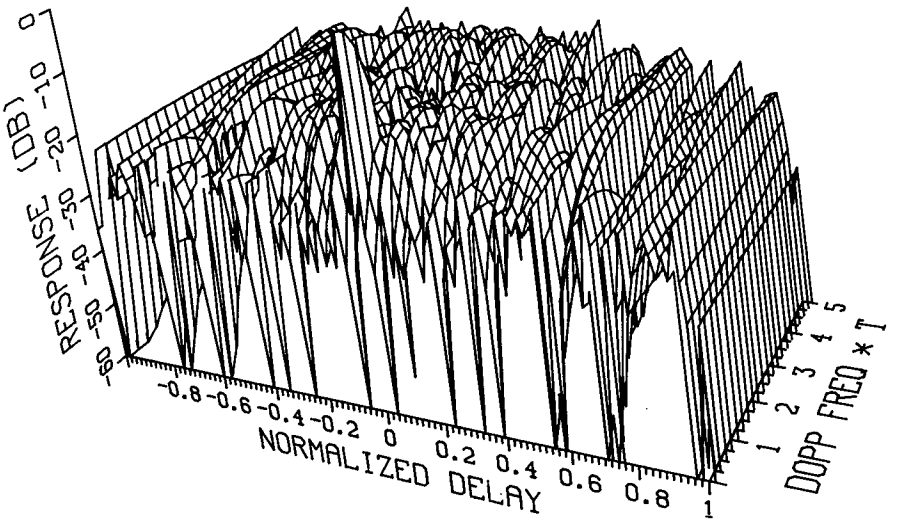

Fig. 9 — Partial ambiguity surface for a 63-element binary shift-register code

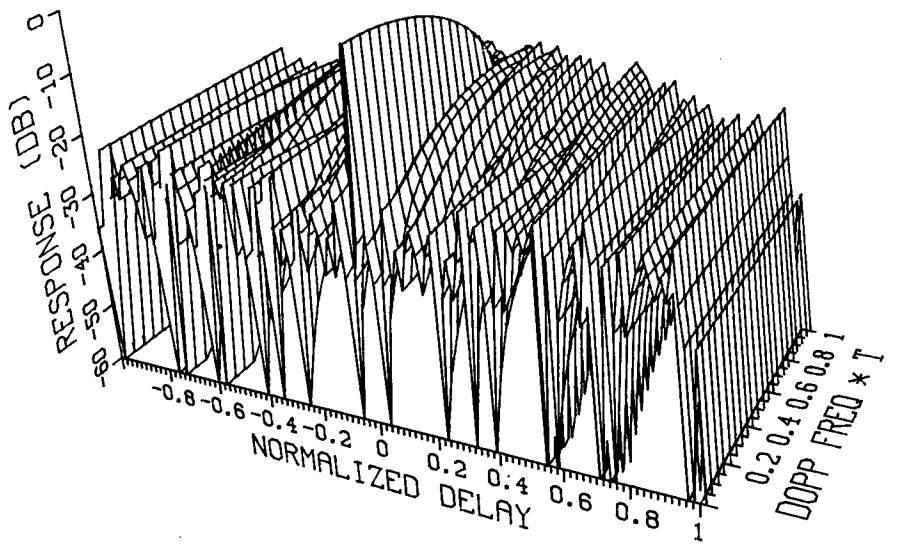

Fig. 10 — Expanded ambiguity surface for a 63-element binary shift-register code

In Fig. 11 we show a cut through the ambiguity surfaces of the three codes at a normalized doppler shift of 0.25, corresponding to a total phase shift across the uncompressed waveform of $\pi/2$ rad. The sample number in the abscissa corresponds to the number of range cells or time intervals whose duration is equal to the subpulse width. By comparing Figs. 11(a) and 11(b) it is seen that for this doppler, the peak sidelobe of the Huffman code is approximately equal to that of the P4 code at approximately −25 dB. For higher doppler, the Huffman-peak sidelobe is larger than the P4 code. The peak sidelobes of the binary code shown in Fig. 11(c) are approximately −19 dB and are not very sensitive to doppler. As described above however, the peak signal in the compressed binary pulse degrades rapidly with increasing doppler as a $(\sin x/x)^2$ function as shown in Figs. 9 and 10.

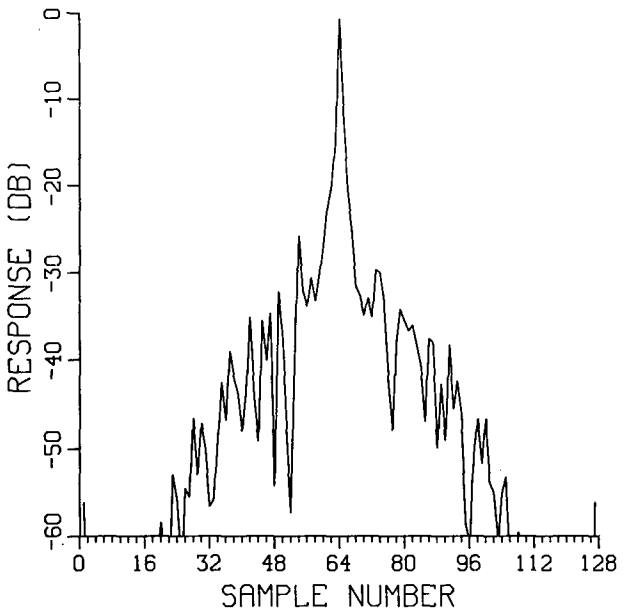

(a) efficient 64-element Huffman code

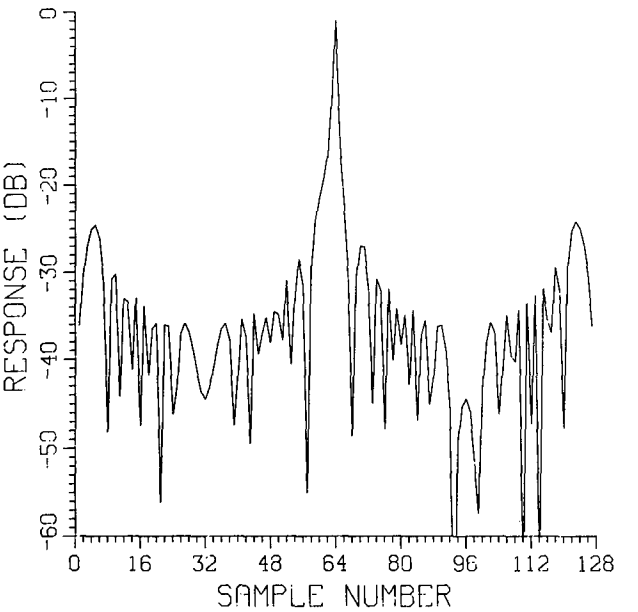

(b) 64-element P4 polyphase code

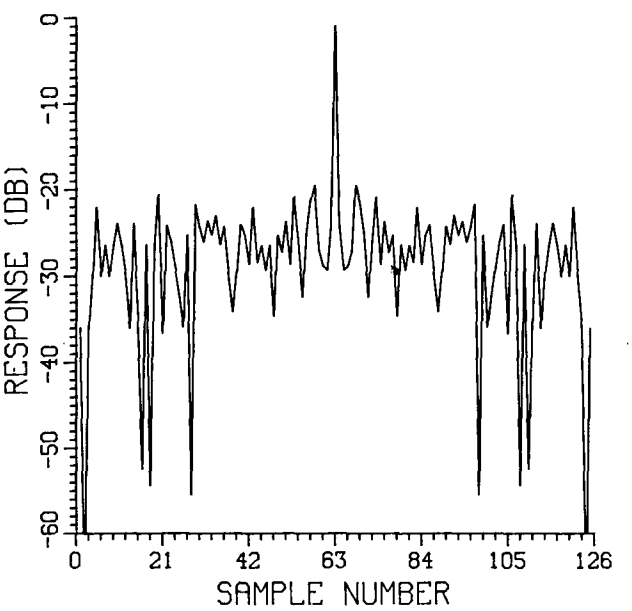

(c) 63-element binary shift-register code

Fig. 11 — Compressed pulses for a normalized doppler shift of 0.25

Another cause of degradation of the Huffman code is errors in generating and compressing the code. The zero sidelobe level, except for the end sidelobes, is an idealization which is not achievable in practice. To assess the sensitivity of the Huffman code to errors, two types of errors were investigated. The first is a random error due to tolerances and the second is due to A/D quantization.

In the first case, an independent random error is added to the inphase I and quadrature Q nominal values for each subpulse. The error is determined from a uniformly distributed sample having a maximum error of $\pm 5\%$ of the nominal value of I or Q. The new I and Q values for each subpulse, denoted by primes, are given by

$$I' = I(1 + e_i)$$

$$Q' = Q(1 + e_q),$$

where e_i and e_q are independent samples from a uniform probability distribution over the range of ± 0.05. An error-free compressed pulse for the efficient 64-element Huffman code is shown in Fig. 12(a), and in Fig. 12(b) a realization is shown for a maximum 5% error imposed on the transmit waveform. It is assumed here that the matched-filter is matched to the transmitted imperfect Huffman waveform. It is seen that the peak sidelobe levels increase to -40 dB over the region where all the sidelobes are zero in the error-free case. An error-free compressed P4 code is shown in Fig. 13(a), and the compressed pulse containing a maximum random error of $\pm 5\%$ is shown in Fig. 13(b). This compressed pulse is seen to be only slightly different from the error-free compressed pulse. Similar results were obtained when the errors were only one way, that is, on either transmit or in the receiver filter.

The effect of quantization errors incurred with the utilization of A/D converters was also simulated for the -36 and -56 dB sidelobe level cases. The results are shown in Fig. 14 for the two-way average and peak sidelobe level vs the number of bits, including the sign bit. From this figure one sees that, as expected, it requires more bits to achieve lower sidelobe levels. Again, the results were nearly the same for the case of a one-way error.

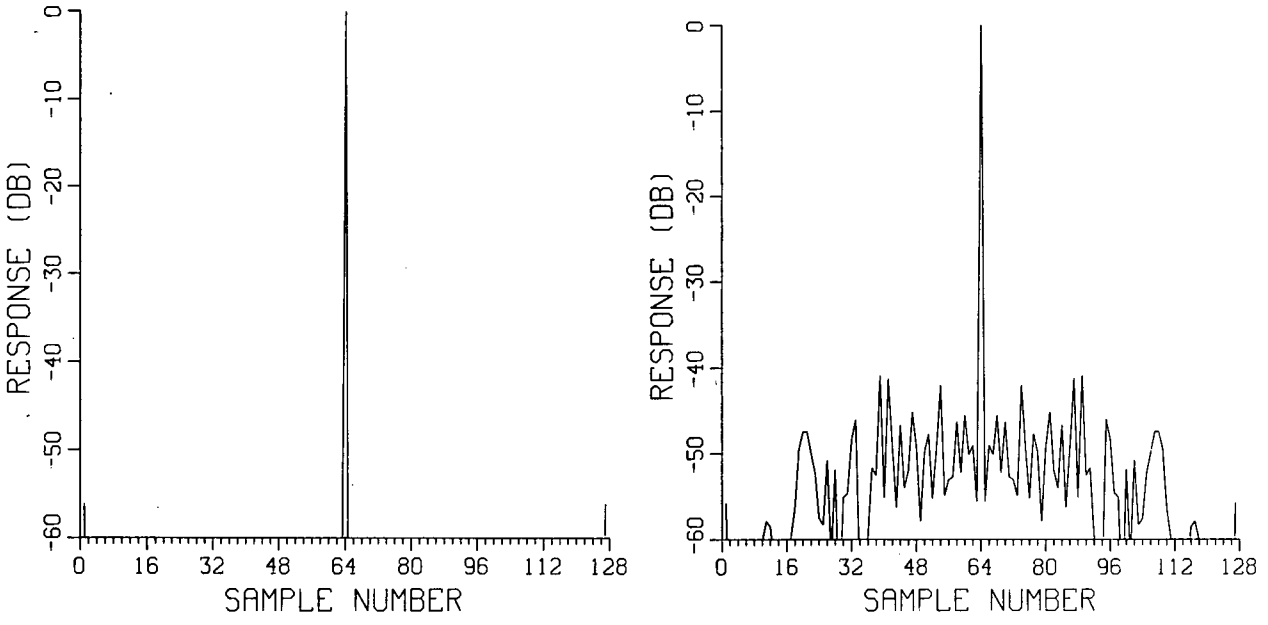

(a) no errors

(b) uniformly distributed random error on each subpulse I and Q values

Fig. 12 — Zero-doppler compressed pulse for an efficient 64-element Huffman code

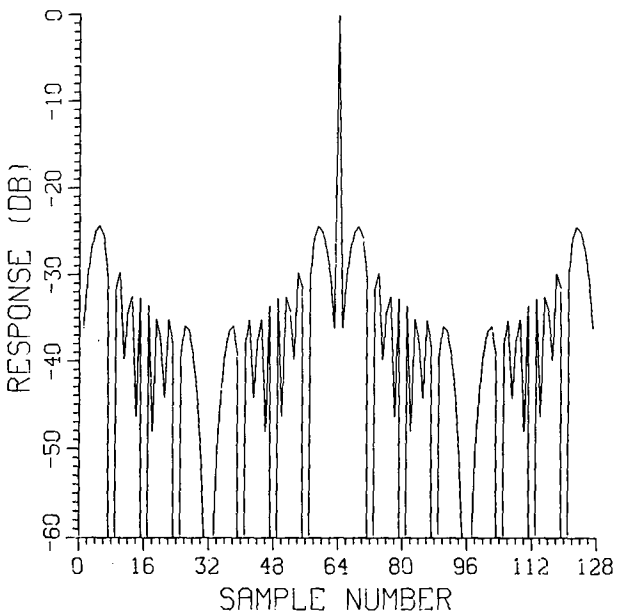

(a) no errors

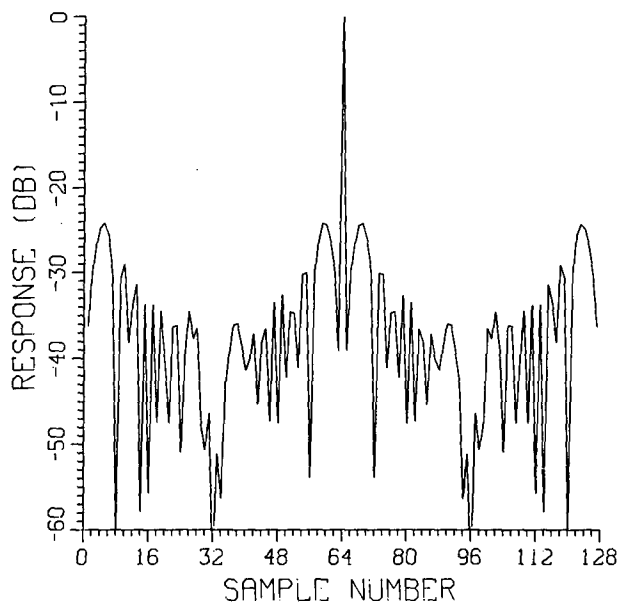

(b) uniformly distributed random error on each subpulse I and Q values

Fig. 13 — Zero-doppler compressed pulse for 64-element P4 polyphase code

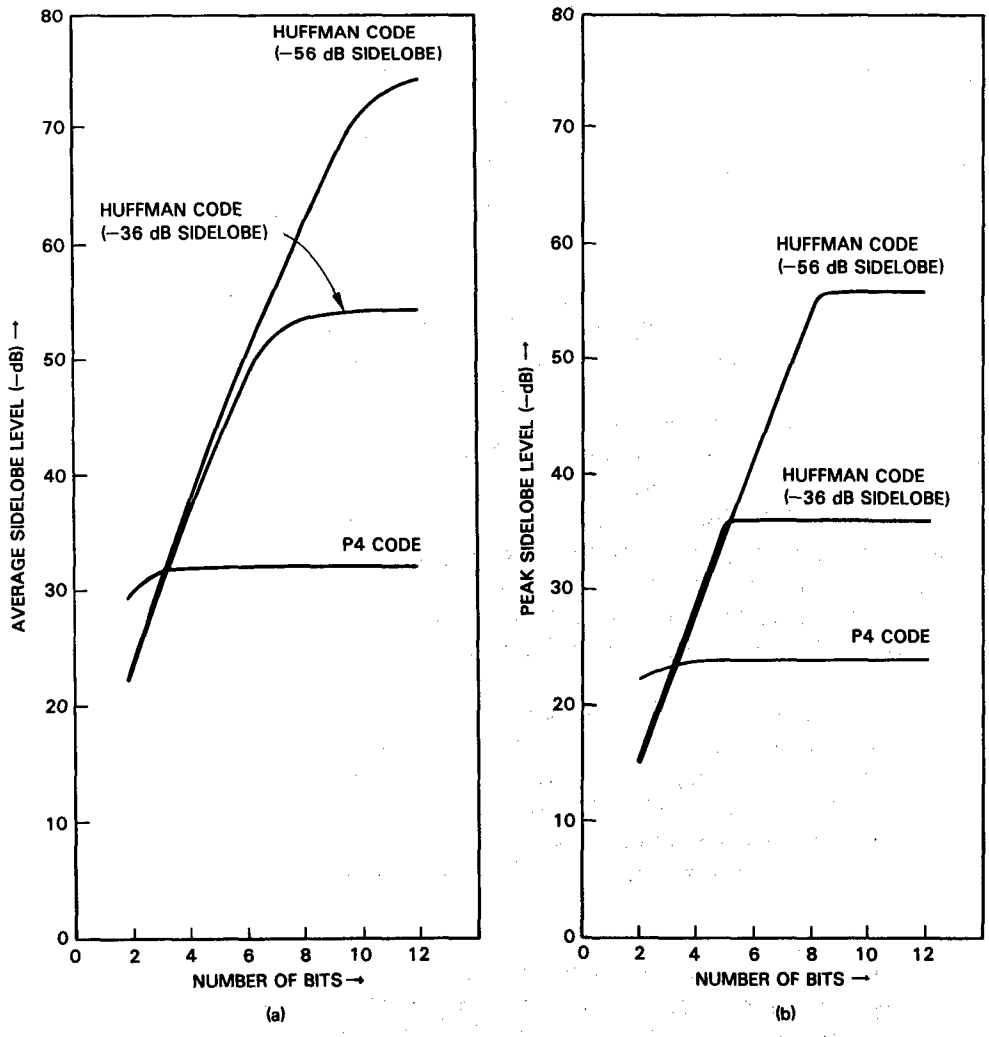

Fig. 14 — Normalized sidelobe levels for the compressed pulse of an efficient 64-element Huffman-coded waveform and a 64-element P4-coded waveform vs the number of A/D bits: (a) average sidelobe level; (b) peak sidelobe level

SUMMARY AND CONCLUSIONS

Relationships of the z-plane zeros of pulse compression waveforms have been reviewed. It was shown how a waveform compressed with a matched filter has an output pulse whose z-plane zeros occur in pairs occurring at the same angle and which are reciprocally related in amplitude. For an N-element input waveform, there are $N-1$ such zero pairs. A synthesis procedure then consists of selecting one zero from each pair. The remaining zeros then correspond to the zeros of the matched filter.

In general, determination of the zeros of the compressed pulse requires factorization of a polynomial of degree $2(N-1)$ in z. However, for the idealized Huffman-coded waveform, the compressed pulse consists of only the central peak and zero sidelobes except for those at either end of the compressed pulse. The consequence is that the z-plane polynomial is quadratic in the variable $z^{-(N-1)}$ so that it can be easily factored. The result is that the zeros lie on two circles, which are reciprocal in amplitude and whose radii depend on the specified sidelobe level, and these zeros also lie on radial lines at regularly spaced intervals of $2\pi/(N-1)$ rad. Random selection of the zeros of the compressed pulse to determine the input waveform usually results in an inefficient waveform in terms of the

of the waveform energy compared to the maximum that could be transmitted. Techniques for improving the efficiency by imparting a large FM content of the waveform were discussed. These methods, based on the work of Schroeder and Ackroyd, were shown to result in a much more efficient waveform. Ackroyd suggested an additional improvement in the waveform efficiency by varying the specified sidelobe design level for a given fixed initial phase angle. We have shown that the efficiency could be further improved by also varying the initial phase angle of the FM-phase characteristic used in determining the zero locations.

The effects of doppler shifts were investigated and it was shown that the zero sidelobes of the Huffman-compressed-pulse increase rapidly with doppler. Ambiguity diagrams were presented for the exemplar 64-element Huffman code, a P4 polyphase code, and a binary shift-register code. Above a normalized doppler shift of approximately 0.25, corresponding to a total phase shift across the uncompressed pulse of $\pi/2$ rad, the peak sidelobes of the 64-element Huffman code exceed those of the 64-element polyphase code. A doppler shift of 0.25 corresponds, for example, to a Mach 1.7 target for a 1 GHz radar having an uncompressed pulse width equal to 64 μs. The sidelobes of the binary code are higher than those of the P4 code and they, as well as those of the P4 code, remain relatively constant with increasing doppler shift. However, the central peak of the binary-coded waveform falls off as a $(\sin \pi fT/\pi fT)^2$ function with the normalized doppler shift fT. For higher pulse compression ratios, it is expected that the sidelobes of the Huffman code would exceed those of the polyphase code for smaller fT because of the lower sidelobes of the P4 code.

The sensitivity of the 64-element Huffman code to random errors and to A/D quantization errors was investigated. It was found that the idealized zero-level sidelobes increased to approximately the -40 dB level in the presence of independent random errors which were a maximum of $\pm 5\%$ of the nominal I and Q channel values for each subpulse. An investigation of the effects of the number of bits used in an A/D converter showed that, to maintain the low sidelobe levels, it is necessary to utilize additional bits. The sidelobe level was found to diminish approximately 7 dB per additional bit.

In conclusion, it is found that the Huffman codes, which are theoretically idealized waveforms in terms of zero sidelobes except for the end sidelobes, degrade rapidly in the presence of doppler shifts. The sidelobes also degrade in the presence of tolerance errors and an insufficient number of A/D bits. The efficiency factor of the Huffman codes may also be an important consideration. For example, for a Huffman code having an efficiency of 50%, there is an approximately 15% reduction in the detection range of the radar.

In view of the foregoing comments, the Huffman waveforms appear to have the most appeal in sufficiently low, or compensated doppler applications where low sidelobes are achievable. The tradeoffs are generally a reduction in range performance, depending on the code efficiency, increased transmitter complexity, and providing the necessary number of A/D bits to support the sidelobe levels. Depending on the code and radar, this number of bits may not need to be greater than what is normally required for proper radar operation.

REFERENCES

1. D.A. Huffman, "The Generation of Impulse-Equivalent Pulse Trains," *IRE Trans. on Information Theory* **IT-8**, S10-S16 (Sept. 1962).

2. C.E. Cook and M. Bernfeld, *Radar Signals* (Academic Press, New York, 1967).

3. M.H. Ackroyd, "The Design of Huffman Sequences," *IEEE Trans. Aerospace and Electronic Systems* **AES-6** (6), 790-796 (Nov. 1970).

4. M.H. Ackroyd, "Amplitude and Phase Modulated Pulse Trains for Radar," *The Radio and Electronic Engineer* **41** (12), 541-552 (1971).

5. M.H. Ackroyd, "Synthesis of Efficient Huffman Sequences," *IEEE Trans. Aerospace and Electronic Systems* **AES-8** (1), 1-8 (Jan. 1972).

6. M.H. Ackroyd, "Computing the Coefficients of High-Order Polynomials," *Electronics Letters* **6**, 715-717 (Oct. 1970).

7. S.W. Golomb and R.R. Scholtz, "Generalized Barker Sequences," *IEEE Trans. Information Theory* **IT-11** (4), 533-537 (Oct. 1965).

8. M.R. Schroeder, "Synthesis of Low-Peak-Factor Signals and Binary Sequences with Low Autocorrelation," *IEEE Trans. Information Theory* **IT-16**, 85-89 (Jan. 1970).

9. B.L. Lewis and F.F. Kretschmer, Jr., "Linear Frequency Modulation Derived Polyphase Pulse Compression Codes," *IEEE Trans. Aerospace and Electronic Systems* **AES-18** (5), 637-641 (Sept. 1982).

10. F.F. Kretschmer, Jr. and B.L. Lewis, "Doppler Properties of Polyphase Coded Pulse Compression Waveforms," *IEEE Trans. Aerospace and Electronic Systems* **AES-19** (4), 521-531 (July 1983).